BIOCHEMISTRY
including biophysical chemistry & molecular biology

ARTICLE

pubs.acs.org/biochemistry

Structure of the HIV-1 5′ Untranslated Region Dimer Alone and in Complex with Gold Nanocolloids: Support of a TAR−TAR-Containing 5′ Dimer Linkage Site (DLS) and a 3′ DIS−DIS-Containing DLS

Jesper Pallesen*

Howard Hughes Medical Institute, Department of Biochemistry and Molecular Biophysics, Columbia University, New York, New York 10032, United States

ABSTRACT: The formation of a genomic RNA dimer is critical for the HIV-1 replication cycle, and dimerization is known to initiate within the 5′UTR (5′ untranslated region) of the viral RNA. However, the 5′UTR constitutes the 335 terminal nucleotides, and because of this considerable size, it has been difficult to study the global structure using conventional structural methods. Here, the atomic force microscope has been used to directly visualize the dimer formed from RNAs including HIV-1 nucleotides 1−744. Gold nanocolloids were deposited on the primer binding site regions in the dimer as an internal control. The dimer showed distinct ring morphology with up to two gold nanocolloids deposited within the ring and one or two strands extending from the ring. This morphology implies a dimer including a DIS-DIS (dimerization initiation site)-containing 3′ dimer linkage site (DLS) and a TAR-TAR (trans-activation region)-containing 5′DLS. Furthermore, the dimer was formed under the influence of Mg^{2+} and was imaged with an atomic force microscope under buffer conditions. The overall ring morphology containing a 5′DLS and a 3′DLS with one or two strands extending from it was conserved in these atomic force microscopy images. This indicates that the observed dimer morphology is physiologically significant. Moreover, evidence of multiple dimer interstrand contacts downstream of the major splice donor were observed, which indicates a component in the selection of full-length genomic RNA in dimer formation during virion packaging.

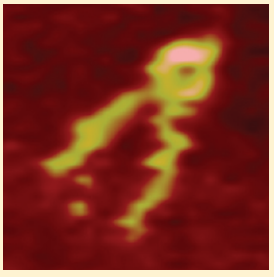

In the HIV-1 replication cycle, several processes such as reverse transcription, transcription, genomic packaging, and genomic dimerization are regulated, at least in part, by cis elements present in the 5′ untranslated region (5′UTR). These elements are named according to their proposed regulatory functions: the trans-activation region (TAR), the 5′ polyadenylation signal [poly(A)], the primer binding site (PBS), the dimerization initiation site (DIS), the major splice donor (SD), and the packaging signal (PSI).[1−3]

In particular, prior to virion packaging, the dimerization of identical, or nearly identical, genomic RNAs must take place.[4] Early EM studies of viral RNA dimers revealed a seemingly parallel strand arrangement with contact in a dimer linkage site (DLS) situated near the 5′ end.[5,6] It was soon established that in vitro transcribed RNAs containing DLS sequence from the 5′UTR dimerized spontaneously in the absence of protein.[7−9] In particular, a six-nucleotide palindromic sequence present in the loop of a hairpin in the 5′UTR was identified as the primary DIS.[10−12] However, dimerization can take place in the absence of DIS function, suggesting other secondary elements are facilitating dimerization, as well.[13−19]

It has been demonstrated that the 5′UTR can adopt alternative conformations.[20,21] In one conformation, the long distance interaction (LDI), the DIS hairpin is disrupted and its sequence involved in alternative base pairings. An alternative conformer, the branched multiple hairpin (BMH), contains an intact DIS hairpin and is dimerization competent. This suggests that the control of the LDI−BMH equilibrium might constitute a regulatory dimerization switch. This switch is under the influence of the viral nucleocapsid protein (NCp7), which has a potent chaperone effect and shifts the conformational equilibrium toward BMH, thereby facilitating genome dimerization.[21] In general, NC exhibits nucleic acid binding, and the interaction can lead to destabilization of nucleic acid structures as well as to strand annealing.[22−26]

HIV-1 5′UTR RNAs in the BMH conformation exposing their DIS hairpins are thought to engage in a kissing loop complex, thereby initiating genome dimerization.[10,12] Rearrangements in the RNA structure are then proposed as a prerequisite for maturation of the kissing loop complex into a more stable extended duplex. NC protein also facilitates the progression from kissing loop complex to extended duplex.[11,27−30]

Other 5′UTR secondary structure candidates to be involved as dimerization facilitators are the TAR and the poly(A) hairpins. They both harbor palindromic sequences potentially capable of participating in kissing loop formation.[13] Biochemical evidence of a conserved 10-nucleotide palindromic sequence in the TAR hairpin involved in kissing loop formation has been reported,[31] and the TAR−TAR interaction has been demonstrated in HIV-1-transfected cell cultures (Cos-7 and HeLa) to be even more important in dimerization of full-length genomic RNAs than the DIS−DIS interaction.[32] Another study suggests the poly(A) hairpin to be involved in interstrand base pairing.[33] The latter study is, however, open for dispute in light of the former two,

Received: April 1, 2011
Revised: June 10, 2011
Published: June 13, 2011

because the poly(A) palindrome had no effect on dimerization in cell culture studies.[32,34]

In this study, AFM is used to explore different aspects of HIV-1 genome dimerization. As model RNA, a 744-nucleotide HIV-1 transcript containing the total 5′UTR and the 5′ part of the Gag open reading frame was used. Dimers were formed from these transcripts, and gold nanocolloid-conjugated primers were annealed to the PBS region as internal markers. These complexes were studied by AFM, and from the images collected, it was possible to, using knowledge of the PBS position in the RNA, infer the existence of at least two interstrand contacts, the 5′DLS and the 3′DLS.

The results support a model in which the 5′DLS contains a TAR−TAR kissing loop interstrand interaction and the 3′DLS contains the DIS−DIS kissing loop interstrand interaction, and it suggests the existence of multiple interstrand interactions downstream of the SD site.

EXPERIMENTAL PROCEDURES

Gold Nanocolloid Coating and Upconcentration. Five nanometer gold nanocolloids were coated with bis(*p*-sulfonatophenyl)phenylphosphine (Strem Chemicals, Newburyport, MA).[35] Six milligrams of bis(*p*-sulfonatophenyl)phenylphosphine was added to 10 mL of a 5 nm gold nanocolloid stock solution (Ted Pella, Redding, CA), and the solution was stirred at room temperature overnight. NaCl was added until the Au colloids precipitated. The colloids were pelleted by centrifugation for 30 min at 3000 rpm in a spin bucket rotor at 14 °C. The supernatant was removed, and the gold nanocolloids were resolved in a 1 mg/mL bis(*p*-sulfonatophenyl)phenylphosphine buffer to a final concentration of 0.83 pmol/μL.

DNA Primer and Gold Colloid−Primer Conjugation. In this study, I used a DNA primer complementary to an exposed region in the HIV-1 5′UTR PBS secondary structure. The primer has been described as PBS-DNA elsewhere.[36] The primer used here has an additional 12-nucleotide 3′ linker terminating in a 3′ thiol group (MWG, Ebersberg, Germany) and has in this context been named primer PBS DNA SH.

Fifty picomoles of coated gold nanocolloids was mixed with *X* pmol of primer PBS DNA SH (*X* = 50, 100, 200, 300, or 400) in 50 mM NaCl. The reaction mixtures were incubated at room temperature for 2 h and then run in a 3% agarose gel [0.5× TBE; 50 mM Tris-HCl (pH 7.9), 45 mM borate, and 0.5 mM EDTA]. The colloid−primer complexes were eluted by insertion of a glass fiber matrix with a dialysis membrane behind it into a slit in the gel in front of the band. The complexes were forced into the glass fiber matrix by further electrophoresis; the matrix was recovered and inserted into a 0.5 mL tube with a hole in the bottom. The 0.5 mL tube was then inserted into a 1.5 mL tube, and the gold nanocolloid−PBS DNA SH complexes were eluted by centrifugation for 5 min at 13000 rpm and room temperature.

Plasmid. The plasmid used for transcription of the 744-nucleotide HIV-1 RNA has been described previously.[3]

In Vitro Transcription. For large-scale transcription of the 744-nucleotide RNA containing the full HIV-1 5′UTR and an additional 409 nucleotides of the 5′ Gag ORF, the template was generated by digestion of the plasmid mentioned above with *Bam*HI. RNA transcription was performed by using 2 μg of linearized plasmid in 20 μL reaction mixtures with 80 mM HEPES-KOH (pH 7.5), 25 mM $MgCl_2$, 2 mM spermidine, 20 mM dithiothreitol, 7.5 mM rNTP, 10 units/mL yeast inorganic PPase, 20 units of ribonuclease inhibitor (Promega, Madison, WI), and 2 units of T7 polymerase incubated at 37 °C for 2 h. The samples were then treated with DNaseI for 15 min prior to purification in 4% denaturing polyacrylamide gels.

NCp7. NCp7 protein was a generous gift from J.-L. Darlix. The protein preparation has been described previously.[31]

Formation of the RNA Dimer−PBS DNA SH−Gold Nanocolloid Complex. The eluted purified gold nanocolloid−PBS DNA SH complex had a volume of 10−15 μL. To this aliquot were added 5 pmol of the 744-nucleotide HIV-1 RNAs and a renaturing buffer [20 mM HEPES (pH 7.2) and *X* mM KCl (*X* = 10, 20, 30, 50, 60, or 70)]. The reaction mixtures were heated to 80 °C for 2 min, slowly cooled to room temperature, and stored on ice. NCp7 was added to a concentration of 5 μM, and the reaction mixtures were incubated at 37 °C for 15 min. After incubation, the reaction mixtures were placed on ice for 2 min and then at 25 °C for 2 min. SDS was added to a final concentration of 0.2%, and samples were left at room temperature for 5 min. The NCp7 protein was removed by phenol extraction, with two steps of phenol with 0.1% SDS, one step of phenol and chloroform, and a last step of chloroform. The reconstituted RNA dimer−PBS DNA SH−gold nanocolloid complexes were either run in a 2% agarose gel (0.5× TBE) at 4 °C or used in AFM experiments. For AFM, the samples were diluted to 1 ng/μL in 1× renaturing buffer.

RNA Dimer Formation. Reaction mixtures containing 5 pmol of the 744-nucleotide RNA were heated to 80 °C and slowly cooled to room temperature. Reaction mixtures were exposed to 5 mM $MgCl_2$ and incubated at room temperature for 15 min. These samples were used for AFM under buffer conditions.

AFM. All samples were prepared on freshly cleaved mica surfaces. In the case of RNA dimer−PBS DNA SH−gold nanocolloid complexes, the freshly cleaved mica was immersed for 10 min in a 100 μg/μL spermine solution (Aldrich, St. Louis, MO). The spermine layer was rinsed in RNase free water (Ambion, Austin, TX) and dried in a delicate N_2 stream. Then 1 μL of a 1 ng/μL RNA dimer−PBS DNA SH−gold nanocolloid complex solution was deposited on top of the spermine layer and left to settle for 2 min. The sample was subsequently rinsed with RNase free water, dried in a delicate N_2 stream, and mounted in the atomic force microscope. All AFM images were collected in tapping mode using NSG11 cantilevers [spring constant k = 5.5 N/m, and curvature radius r = 10 nm (NT-MDT, Moscow, Russia)].

For the gold nanocolloid control experiment, spermine-coated mica was prepared as described above. Bis(*p*-sulfonatophenyl)-phenylphosphine-coated gold nanocolloids (described above) were deposited on spermine-coated mica as well as on freshly cleaved mica. In both cases, the specimen was rinsed, dried, and imaged as described above.

For the RNA dimer experiments, the reaction mixture described above was diluted to 1 ng/μL in imaging buffer [30 mM KCl, 5 mM $MgCl_2$, and 10 mM HEPES (pH 7.2)], and 2 μL was immediately deposited onto a freshly cleaved mica surface already mounted in the atomic force microscope. The sample was left to equilibrate for 2 min; a liquid cell was mounted, and imaging buffer was slowly injected into the liquid cell. The AFM images were collected in tapping mode using OMCL-TR400PSA cantilevers [spring constant k = 0.08 N/m, and curvature radius r < 20 nm (Olympus, Atomic Force F&E Gmbh, Mannheim, Germany)].

All AFM images were recorded with a Veeco MultiMode Scanning Probe Microscope equipped with a Nanoscope IIIa

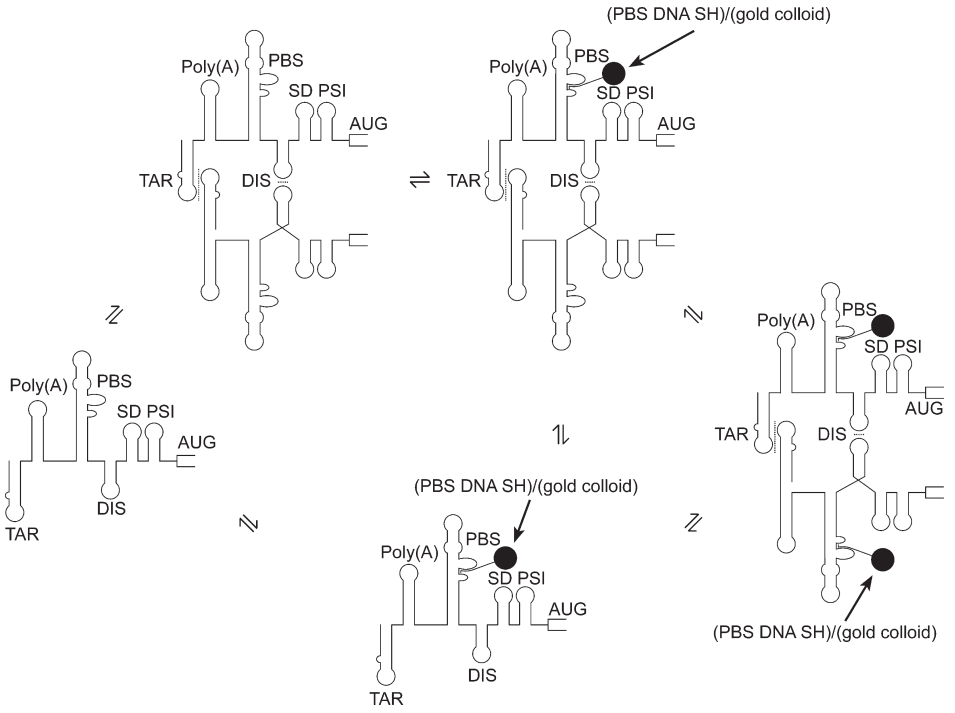

Figure 1. Schematic representation of the formation of RNA dimer−PBS DNA SH−gold nanocolloid complexes from individual components. The final reaction product is a result of several equilibria. As seen, the RNA dimer is expected to exhibit the morphology of a ring with one or two strands emerging. Either zero, one, or two gold nanocolloids are expected to be deposited onto the PBS region inside the ring structure.

controller (Digital Instruments, Santa Barbara, CA). The AFM scanner used was the 10 μm × 10 μm × 2.5 μm "E" scanner. The recorded AFM images were analyzed using the Veeco Multimode version 5.30r1.

Because some rings were slightly distorted, ring diameters were estimated to be $0.5(r_1^2 + r_2^2)^{1/2}$, where r_1 and r_2 are the minor and major axes of the ellipse, respectively.[31]

RESULTS

AFM has proven to be useful for revealing the morphology of biological systems[37] and was reviewed in ref 38. To identify specific primary structures in the HIV-1 5′UTR RNA, markers were specifically attached to the RNA. A DNA primer complementary to an exposed region in the PBS secondary structure in the 5′UTR was designed. The primer targeted part of the major loop in the PBS secondary structure and part of the PAS region previously shown to engage in base pairing with the primer tRNA.[39−42] It also included a linker region terminating in a 3′ thiol. The targeted region in the PBS secondary structure has been shown previously to be accessible to primers,[36] and the primer variant used in this study will be termed PBS DNA SH. Five nanometer gold nanocolloids were chosen for conjugation to the PBS DNA SH 3′ thiol group. The aim was to specifically attach a gold nanocolloid via PBS DNA SH to the 5′UTR PBS region. Figure 1 presents the presumed reaction scheme of the study. HIV-1 5′UTR RNAs in the BMH conformation dimerize via DIS−DIS and TAR−TAR interactions. The annealing of PBS DNA SH results in dimers with zero, one, or two gold nanocolloids attached to the RNA ring formed during dimerization.

Several reaction stoichiometries were included in the search for reaction conditions leading to a distribution of gold nanocolloids with an optimal number of primers attached per colloid.

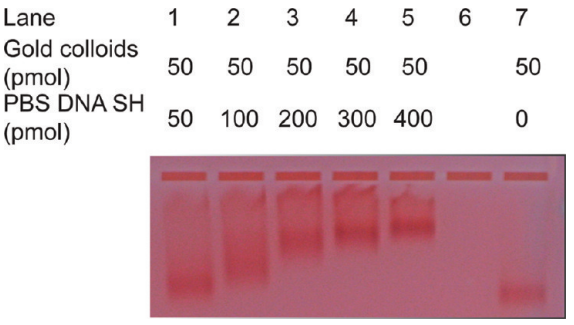

Figure 2. Formation of PBS DNA SH−gold nanocolloid complexes. The increasing shifts in the gel (lanes 1−5) illustrate that increasing the concentration of primer PBS DNA SH relative to the concentration of gold nanocolloids results in more primers attached per colloid. Lane 7 is a control containing gold nanocolloids only.

The optimal PBS DNA SH−gold nanocolloid mix would presumably be able to deposit a gold nanocolloid on the RNA without cross reactivity resulting in RNA multimers.

From the band shifts presented in the gel in Figure 2, it is evident that with the increase in the amount of primer in the reaction mixture it was possible to attach a larger number of primers per gold nanocolloid.

The next step was to dimerize the 744-nucleotide RNA transcript containing the entire HIV-1 5′UTR (nucleotides 1−335) and the 5′ part of the Gag open reading frame (nucleotides 336−744) and attach the purified PBS DNA SH−gold nanocolloids species to the PBS target sequence. Gel analyses showed that the PBS DNA SH: gold nanocolloid stoichiometry resulting in the desired Au nanocolloid deposition with no formation of RNA−multimer complexes was 4:1 (data not shown and Figure 2, lane 3).

dx.doi.org/10.1021/bi200488h |*Biochemistry* 2011, 50, 6170–6177

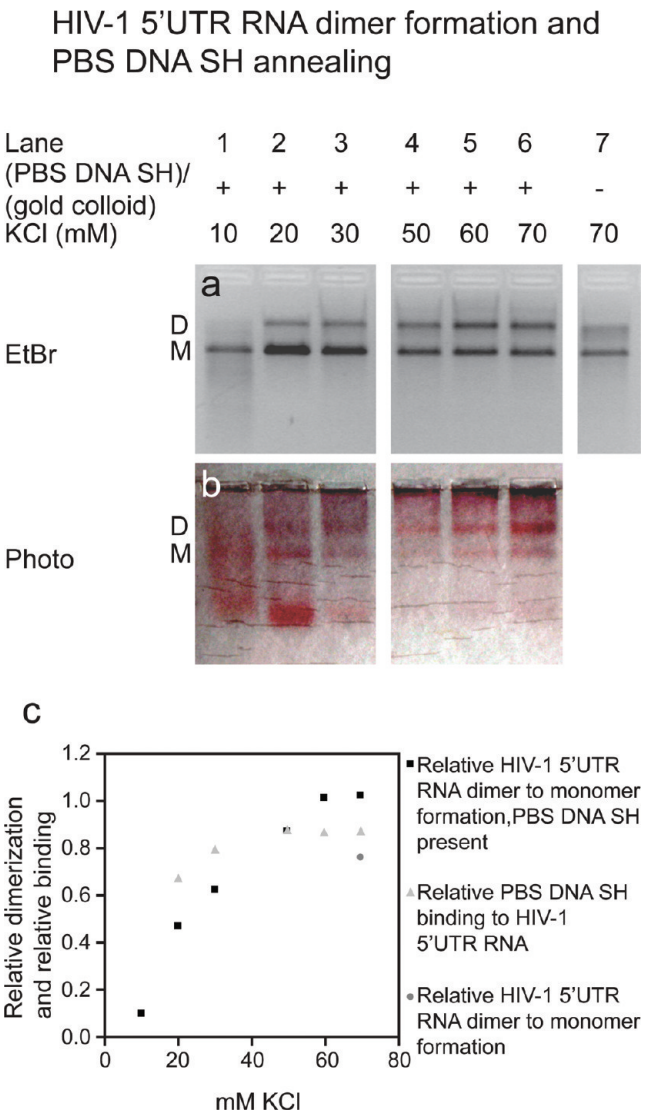

Figure 3. RNA dimer formation and attachment of PBS DNA SH−gold nanocolloid complexes to the 5′UTR PBS region. (a) RNA dimerization as a function of KCl concentration. Lanes 1−6 show dimerization in the presence of PBS DNA SH−gold nanocolloid complexes. Lane 7 is a control showing RNA dimerization with no PBS DNA SH−gold nanocolloid complex added. (b) Annealing of PBS DNA SH−gold nanocolloid complexes to the RNA dimerization reaction mixtures shown in panel a. (c) Quantification of RNA dimerization and annealing of the PBS DNA SH−gold nanocolloid complex as a function of KCl concentration. When the KCl concentration becomes low, RNA dimerization and deposition of PBS DNA SH−gold nanocolloid complexes are inhibited. At 70 mM KCl, both RNA dimerization and PBS DNA SH−gold nanocolloid complex deposition reactions have reached a plateau. Because at 10 mM KCl gold nanocolloid deposition has been reduced to an unspecific smear and dimerization has been disrupted (panel b, lane 1), quantification of this lane has been omitted.

RNA dimer−PBS DNA SH−gold nanocolloid complexes were produced. Figure 3 shows the formation of these complexes at KCl concentrations ranging between 10 and 70 mM. Figure 3a illustrates that dimerization is dependent on the concentration of KCl. When the KCl concentration was increased, RNA dimer formation became more efficient and reached a plateau at 60−70 mM KCl (Figure 3a, lanes 6 and 3c). At low (10 mM) KCl concentrations, dimer formation was severely inhibited.

Figure 3b presents the annealing efficiency of the PBS DNA SH−gold nanocolloid complex for the PBS region of the 744-nucleotide RNA. Similarly, it is evident from panels b and c of Figure 3 that the annealing of this primer complex to the RNA is dependent on the presence of KCl. At 10 mM KCl, the annealing was nonfunctional, whereas it reached a plateau in the range of 50−70 mM KCl (Figure 3b, lane 6, and Figure 3c). Because the annealing of the PBS DNA SH−gold nanocolloid complex to RNA has been reduced to an unspecific smear at 10 mM KCl (Figure 2b, lane 1), quantification of this lane has been omitted in Figure 3c. An interesting side effect from having PBS DNA SH−gold nanocolloid complexes present during RNA dimerization is the apparently higher dimer yield (Figure 3, control in lane 7 vs reaction dimer formation in lane 6). This effect probably originates from the fact that the overall molecular concentration is higher when the PBS DNA SH−gold nanocolloid complex is present, making the effective RNA concentration higher.

The reaction mixture containing the RNA dimer−PBS DNA SH−gold nanocolloid complexes in 70 mM KCl was then deposited onto a mica surface precovered with spermine.[37,43] As seen from the AFM images in Figure 4, the molecular assemblies showed ring morphologies with one or two strands extending from the ring. Attached to the rings one finds examples of zero, one, or two gold nanocolloids (Figure 4b−d). The ring diameter was determined from the AFM images to be 43.4 ± 7.0 nm (Figure 4e); deposition of gold nanocolloids did not affect ring diameter. A cross section of the ring structure at the position of the gold nanocolloids is shown in Figure 4f. The measured height of the gold nanocolloids was typically in the range of 1.0−1.5 nm, significantly smaller than the nominal colloid diameter of 5 nm.

To address this discrepancy, I performed a control experiment (data not shown) in which the 5 nm gold nanocolloids were deposited on raw mica and on spermine-coated mica. The measured gold nanocolloid heights were 3.7 ± 0.8 nm (raw mica) and 0.7 ± 0.6 nm (spermine-coated mica).

To validate the physiological significance of the observed dimer morphology, I imaged it under buffer conditions. The dimer was formed by treatment with Mg^{2+} (Figure 5a). As depicted in Figure 5b, the ring morphology with one or two strands extending from it was preserved in the AFM images obtained in buffer. The diameter for the Mg^{2+}-treated dimers imaged in buffer was determined to be 40.3 ± 8.3 nm (Figure 5c).

As mentioned earlier, this AFM study has revealed examples of ring structures from which either one or two strands extend. Figure 6 presents examples of rings from which two strands extend and in which the two strands seem to merge into one further downstream.

DISCUSSION

Dimerization of HIV-1 RNA transcripts (nucleotides 1−744) and annealing of the gold-functionalized PBS DNA SH were performed over a range of KCl concentrations. The reaction is shown schematically in Figure 1. The desired final product of RNA dimers with deposition of gold nanocolloids in the PBS region is dependent on several equilibria; Figure 3 demonstrates that the product yield is dependent on the concentration of KCl. On the basis of the results presented in Figure 3, AFM experiments were performed on RNA dimer−PBS DNA SH−gold

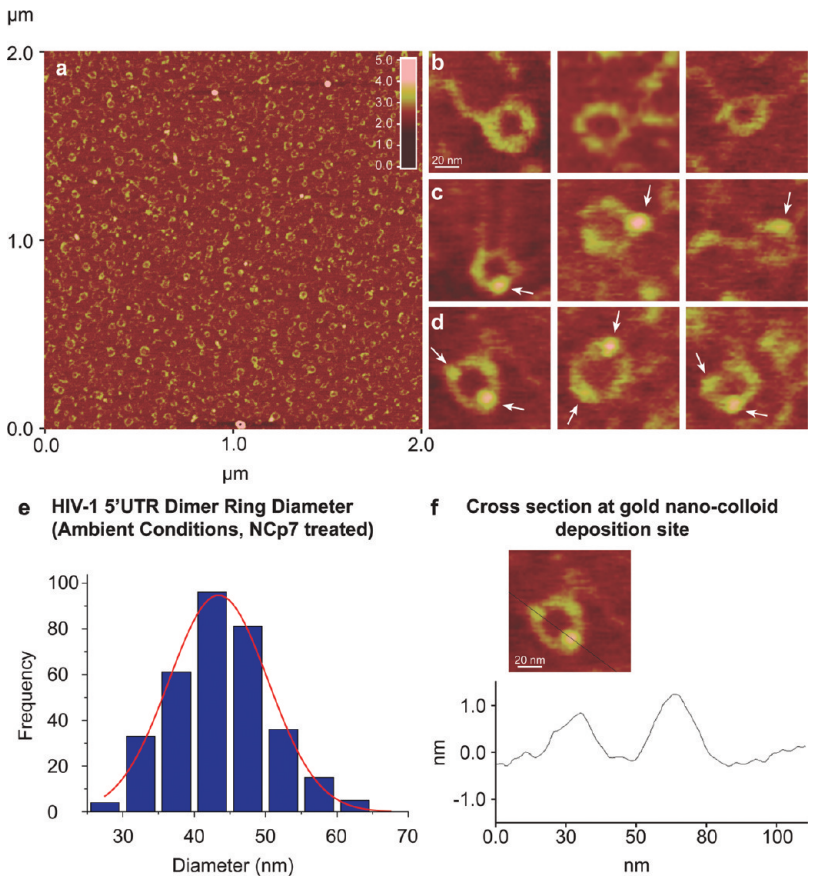

Figure 4. AFM analysis of RNA dimer−PBS DNA SH−gold nanocolloid complexes. The RNA dimer structure is a ring with one or two strands emerging from it. (a) Overview AFM image. (b) RNA dimers with no gold nanocolloids attached. (c) RNA dimers with one gold nanocolloid attached to each ring structure. (d) RNA dimers with two gold nanocolloids attached to each ring structure. Arrows indicate positions of gold nanocolloids. Gold nanocolloids are attached to the 5′UTR PBS region (Figure 1). (e) Distribution of measured ring diameters (43.4 ± 7.0 nm). (f) Cross section of an RNA dimer presenting the profile of the ring at the position of the two attached gold nanocolloids. The data were obtained from three independent experiments.

nanocolloid complexes prepared in 70 mM KCl (both RNA dimerization and gold nanocolloid deposition processes have reached a plateau under these conditions).

Among the RNA dimers in the sample, examples of no gold nanocolloid deposition and of one and two gold nanocolloids are to be expected (Figure 1). Indeed, this is what the AFM images depicted in Figure 4b−d reveal. Moreover, the gold nanocolloids are, as expected, almost entirely observed on the ring structures. At 70 mM KCl, the RNA monomer:dimer ratio is ∼1:1 and ∼80% of the PBS DNA SH−gold nanocolloids complex added to the reaction mixtures have been attached to HIV-1 RNA giving an estimated ∼40% of the RNA being in complex with gold nanocolloids in solution (Figure 3). An estimated 25% of the HIV-1 RNA dimers observed in the AFM experiments have visible gold nanocolloids attached to the PBS region. The slightly lower yield is expected because of additional sample preparation in the latter case (Experimental Procedures). The observed gold nanocolloid height was typically in the range of 1.0−1.5 nm (Figure 4f). This is smaller than expected from colloids with a nominal diameter of 5 nm. From the control experiment, it is seen, however, that the diameter (height) measured with the atomic force microscope of the gold nanocolloids used is 3.7 ± 0.8 nm. When the colloid diameter was measured after deposition on spermine-coated mica [as used in imaging of the RNA dimer−PBS DNA SH−gold nanocolloid complex (see Experimental Procedures)], it turned out to be 0.7 ± 0.6 nm. This effect can be explained by the gold nanocolloids being partly submerged in the soft spermine layer on the mica, and this finding is very consistent with the results obtained from imaging the RNA dimer−PBS DNA SH−gold nanocolloid complex on spermine-coated mica under ambient (i.e., in air) conditions (Figure 4). Hence, it can be concluded that it is possible to specifically attach gold nanocolloids via DNA primers to the PBS region of the HIV-1 5′UTR. Thereby, the position of PBS is directly visible in AFM images, and other structural information can be mapped accordingly.

Upon examination of the dimer structures in Figure 4, it is evident that there are two interstrand contacts, one upstream and one downstream of the PBS. I interpret the downstream interaction, the 3′DLS, as the DIS−DIS interaction, which is indeed expected to be present. The upstream interaction, the 5′DLS, is, however, more intriguing. It seems to be present terminally in the 5′UTR because RNA strands on its upstream side are never observed. Such an interaction has been previously reported, and the TAR hairpin[31,32] and the poly(A) hairpin[33] have been suggested, via their palindromic sequences, to be part of kissing loop interactions. Evidence contradicts the involvement of poly(A),[32,34] and part of its palindromic sequence seems to be involved in a long-range pseudoknot.[44] Moreover, enzymatic

dx.doi.org/10.1021/bi200488h |*Biochemistry* 2011, 50, 6170–6177

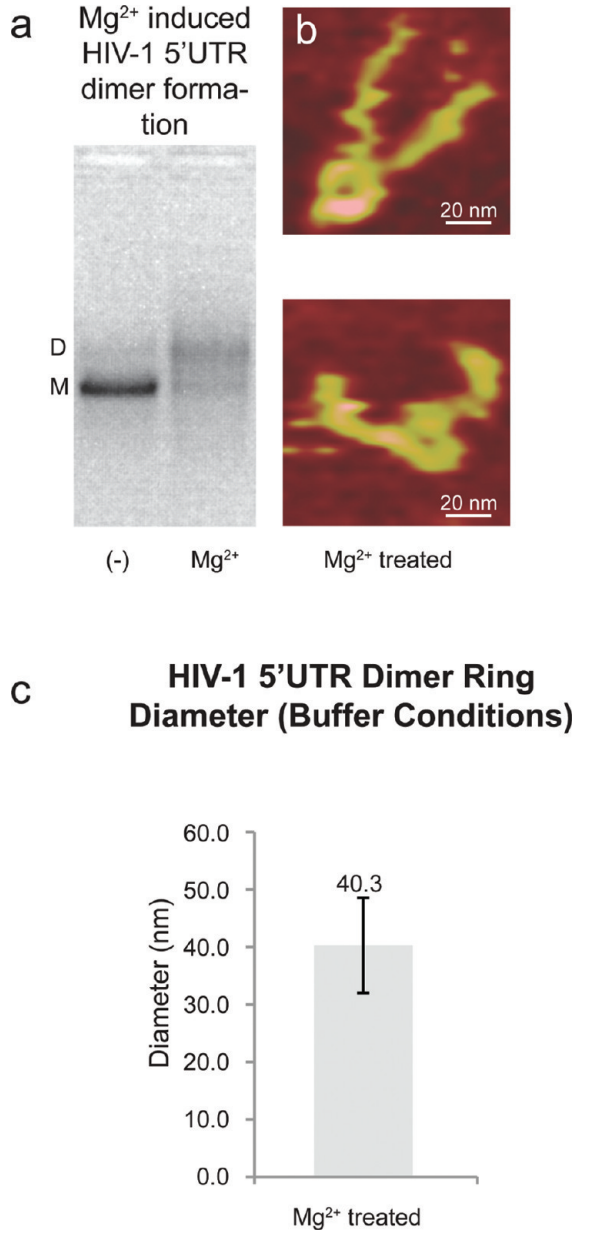

Figure 5. AFM analysis of Mg^{2+}-treated RNA dimers in buffer. (a) Formation of the HIV-1 RNA dimer can be mediated by Mg^{2+} ions. Abbreviations: M, monomer; D, dimer; Mg^{2+}, 5 mM Mg^{2+}; (−), no Mg^{2+}. (b) Ring structure with one or two strands emerging from it observed under ambient conditions preserved for Mg^{2+}-induced RNA dimers imaged in buffer. (c) Measured ring diameters (40.3 ± 8.3 nm). The data were obtained from three independent experiments.

probing of dimers formed from isolated TAR hairpin transcripts supports a TAR−TAR kissing loop interaction.[31] Combined with the proof of a TAR−TAR interaction in HIV-1-transfected cell cultures[32] and the fact that RNA strands are never observed on the upstream side of the 5′DLS, these observations support the interpretation that it contains a TAR−TAR kissing loop interaction. Because the TAR stem−loop sequence is positioned at the 5′ terminus (nucleotides 1−57), this interpretation is fully consistent with the AFM images obtained. In addition, dual kissing loop interactions in the 5′UTR of a related retrovirus (MoMuLV) have been observed.[45]

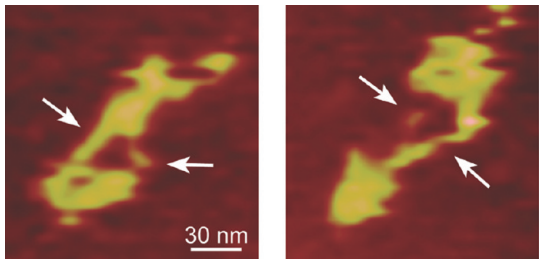

Figure 6. RNA dimers showing two strands emerging from its ring structure. The two strands seem to merge into one further downstream. Arrows indicate strands emerging from the ring structure.

The ring diameter distribution as revealed from the AFM images under ambient scan conditions is depicted in Figure 4e, and the diameter was determined to be 43.4 ± 7.0 nm. Hoglund et al. report EM structures with similar diameters varying from 13 to 40 nm with only one example below 30 nm.[33] This corresponds very well with the results obtained here.

Because the observed 5′UTR RNA dimer structure was imaged under ambient conditions, it was of interest to validate the physiological relevance by imaging it under buffer conditions. RNA dimers were produced by treatment with Mg^{2+} ions and verified in gels (Figure 5a). The gold nanocolloid labeling was not possible in the buffer experiments; Mg^{2+} had to be part of the buffer to attach the RNA dimer to the mica surface, and divalent cations made the protected gold nanocolloids precipitate irreversibly. The AFM buffer results are depicted in Figure 5, and it is seen that the dimer morphology observed under ambient AFM imaging conditions, depicted in Figure 4, was preserved (Figure 5b). Furthermore, the ring diameter observed for the Mg^{2+}-treated dimers in buffer [40.3 ± 8.3 nm (Figure 5c)] was very consistent with the diameter observed for the dimer structure under ambient conditions [43.4 ± 7.0 nm (Figure 4e)]. It is thus concluded that the observed overall 5′UTR morphology including a TAR−TAR-containing 5′DLS and a DIS−DIS-containing 3′DLS is likely to be physiologically significant.

During packaging of HIV-1 virions, the virus is capable of discriminating between full-length genomic RNA dimers and other RNA species because only full-length genomic RNA dimers are found in virions. Thus, one might assume that sequences downstream the SD might be involved in dimer formation, too. Indeed, the PSI secondary structure is present downstream of SD. Upon further examination of Figures 4 and 5, it is evident that there is always one or two strands extending from the ring structure. In the case of two strands, the explanation is rather trivial. In both RNA strands involved in the dimer, nucleotides 278−744 are found downstream of the DIS hairpin. However, when only one strand is observed to extend from the ring structure, it could be either because only one of the two strands is attached to the mica surface or because there are multiple interactions between the strands. Indeed, Figure 6 shows examples of two strands emerging from the ring structure, and further downstream they merge into one. Taken together with the many examples of only one strand emerging from the ring structure, this may be interpreted as evidence of multiple interactions between the strands in the HIV-1 genomic dimer downstream of the SD. Such interactions have previously been reported in related viruses.[46,47]

In conclusion, the structure of dimerized HIV-1 RNAs corresponding to nucleotides 1−744 has been investigated via AFM. It was possible to specifically deposit gold nanocolloids to the PBS

region via DNA primers and thereby directly identify the PBS position in the AFM images. This proves that DNA−gold chemistry can be a valuable tool in future AFM studies of native nucleic acid structures. This knowledge allowed the resulting ring morphologies with one or two strands emerging from them to be interpreted as dimers including a TAR−TAR-containing 5′DLS and a DIS−DIS-containing 3′DLS. The dimer structure was validated under buffer conditions that were close to physiological conditions, which strongly suggests the observed dimer structure is biologically significant. Finally, evidence suggesting multiple HIV-1 RNA interstrand interactions downstream of the 5′UTR major splice donor was observed in the AFM images, suggesting this is part of the mechanism by which only full-length genomic RNAs are incorporated into dimers during packaging of new virions.

AUTHOR INFORMATION

Corresponding Author

*Howard Hughes Medical Institute, Department of Biochemistry and Molecular Biophysics, Columbia University, 650 W. 168th St., BB2-221, New York, NY 10032. Phone: (212) 305-9521. Fax: (212) 305-9500. E-mail: jp2854@columbia.edu.

Funding Sources

I am grateful of the financial support given to the Interdisciplinary Nanoscience Center and the Center for DNA Technology from the Danish Research Councils, the Danish National Research Foundation and the Carlsberg Foundation.

ACKNOWLEDGMENT

I acknowledge The Department of Molecular Biology, the Interdisciplinary Nanoscience Center, and the Center for DNA Technology at the University of Aarhus for technical assistance.

ABBREVIATIONS

AFM, atomic force microscopy; BMH, branched multiple hairpin; DIS, dimerization initiation site; DLS, dimer linkage site; Gag, group-specific antigen; LDI, long distance interaction; MoMuLV, Moloney murine leukemia virus; NC, nucleocapsid protein; ORF, open reading frame; PAS, primer activation signal; PBS, primer binding site; poly(A), 5′ polyadenylation signal; PSI, packaging signal; SD, major splice donor; TAR, trans-activation region; 5′UTR, 5′ untranslated region.

REFERENCES

(1) Berkhout, B. (2000) Multiple Biological Roles Associated with the Repeat (R) Region of the HIV-1 RNA Genome. *Adv. Pharmacol. 48*, 29–73.

(2) Berkhout, B. (1996) Structure and Function of the Human Immunodeficiency Virus Leader RNA. *Prog. Nucleic Acid Res. Mol. Biol. 54*, 1–34.

(3) Damgaard, C. K., Andersen, E. S., Knudsen, B., Gorodkin, J., and Kjems, J. (2004) RNA Interactions in the 5′ Region of the HIV-1 Genome. *J. Mol. Biol. 336*, 369–379.

(4) Sakuragi, J., Sakuragi, S., and Shioda, T. (2007) Minimal Region Sufficient for Genome Dimerization in the Human Immunodeficiency Virus Type 1 Virion and its Potential Roles in the Early Stages of Viral Replication. *J. Virol. 81*, 7985–7992.

(5) Bender, W., and Davidson, N. (1976) Mapping of Poly(A) Sequences in the Electron Microscope Reveals Unusual Structure of Type C Oncornavirus RNA Molecules. *Cell 7*, 595–607.

(6) Kung, H. J., Hu, S., Bender, W., Bailey, J. M., Davidson, N., Nicolson, M. O., and McAllister, R. M. (1976) RD-114, Baboon, and Woolly Monkey Viral RNA's Compared in Size and Structure. *Cell 7*, 609–620.

(7) Darlix, J. L., Gabus, C., Nugeyre, M. T., Clavel, F., and Barre-Sinoussi, F. (1990) Cis Elements and Trans-Acting Factors Involved in the RNA Dimerization of the Human Immunodeficiency Virus HIV-1. *J. Mol. Biol. 216*, 689–699.

(8) Marquet, R., Baudin, F., Gabus, C., Darlix, J. L., Mougel, M., Ehresmann, C., and Ehresmann, B. (1991) Dimerization of Human Immunodeficiency Virus (Type 1) RNA: Stimulation by Cations and Possible Mechanism. *Nucleic Acids Res. 19*, 2349–2357.

(9) Marquet, R., Paillart, J. C., Skripkin, E., Ehresmann, C., and Ehresmann, B. (1994) Dimerization of Human Immunodeficiency Virus Type 1 RNA Involves Sequences Located Upstream of the Splice Donor Site. *Nucleic Acids Res. 22*, 145–151.

(10) Laughrea, M., and Jette, L. (1994) A 19-Nucleotide Sequence Upstream of the 5′ Major Splice Donor is Part of the Dimerization Domain of Human Immunodeficiency Virus 1 Genomic RNA. *Biochemistry 33*, 13464–13474.

(11) Laughrea, M., and Jette, L. (1996) Kissing-Loop Model of HIV-1 Genome Dimerization: HIV-1 RNAs can Assume Alternative Dimeric Forms, and all Sequences Upstream Or Downstream of Hairpin 248−271 are Dispensable for Dimer Formation. *Biochemistry 35*, 1589–1598.

(12) Skripkin, E., Paillart, J. C., Marquet, R., Ehresmann, B., and Ehresmann, C. (1994) Identification of the Primary Site of the Human Immunodeficiency Virus Type 1 RNA Dimerization in Vitro. *Proc. Natl. Acad. Sci. U.S.A. 91*, 4945–4949.

(13) Berkhout, B., and van Wamel, J. L. (1996) Role of the DIS Hairpin in Replication of Human Immunodeficiency Virus Type 1. *J. Virol. 70*, 6723–6732.

(14) Clever, J. L., and Parslow, T. G. (1997) Mutant Human Immunodeficiency Virus Type 1 Genomes with Defects in RNA Dimerization Or Encapsidation. *J. Virol. 71*, 3407–3414.

(15) Haddrick, M., Lear, A. L., Cann, A. J., and Heaphy, S. (1996) Evidence that a Kissing Loop Structure Facilitates Genomic RNA Dimerisation in HIV-1. *J. Mol. Biol. 259*, 58–68.

(16) Laughrea, M., Jette, L., Mak, J., Kleiman, L., Liang, C., and Wainberg, M. A. (1997) Mutations in the Kissing-Loop Hairpin of Human Immunodeficiency Virus Type 1 Reduce Viral Infectivity as Well as Genomic RNA Packaging and Dimerization. *J. Virol. 71*, 3397–3406.

(17) Sakuragi, J. I., and Panganiban, A. T. (1997) Human Immunodeficiency Virus Type 1 RNA Outside the Primary Encapsidation and Dimer Linkage Region Affects RNA Dimer Stability in Vivo. *J. Virol. 71*, 3250–3254.

(18) Shen, N., Jette, L., Liang, C., Wainberg, M. A., and Laughrea, M. (2000) Impact of Human Immunodeficiency Virus Type 1 RNA Dimerization on Viral Infectivity and of Stem-Loop B on RNA Dimerization and Reverse Transcription and Dissociation of Dimerization from Packaging. *J. Virol. 74*, 5729–5735.

(19) Shen, N., Jette, L., Wainberg, M. A., and Laughrea, M. (2001) Role of Stem B, Loop B, and Nucleotides Next to the Primer Binding Site and the Kissing-Loop Domain in Human Immunodeficiency Virus Type 1 Replication and Genomic-RNA Dimerization. *J. Virol. 75*, 10543–10549.

(20) Abbink, T. E., and Berkhout, B. (2003) A Novel Long Distance Base-Pairing Interaction in Human Immunodeficiency Virus Type 1 RNA Occludes the Gag Start Codon. *J. Biol. Chem. 278*, 11601–11611.

(21) Huthoff, H., and Berkhout, B. (2001) Two Alternating Structures of the HIV-1 Leader RNA. *RNA 7*, 143–157.

(22) Dib-Hajj, F., Khan, R., and Giedroc, D. P. (1993) Retroviral Nucleocapsid Proteins Possess Potent Nucleic Acid Strand Renaturation Activity. *Protein Sci. 2*, 231–243.

(23) Khan, R., and Giedroc, D. P. (1992) Recombinant Human Immunodeficiency Virus Type 1 Nucleocapsid (NCp7) Protein Unwinds tRNA. *J. Biol. Chem. 267*, 6689–6695.

(24) Prats, A. C., Sarih, L., Gabus, C., Litvak, S., Keith, G., and Darlix, J. L. (1988) Small Finger Protein of Avian and Murine Retroviruses has

Nucleic Acid Annealing Activity and Positions the Replication Primer tRNA Onto Genomic RNA. *EMBO J. 7*, 1777–1783.

(25) Tsuchihashi, Z., and Brown, P. O. (1994) DNA Strand Exchange and Selective DNA Annealing Promoted by the Human Immunodeficiency Virus Type 1 Nucleocapsid Protein. *J. Virol. 68*, 5863–5870.

(26) You, J. C., and McHenry, C. S. (1994) Human Immunodeficiency Virus Nucleocapsid Protein Accelerates Strand Transfer of the Terminally Redundant Sequences Involved in Reverse Transcription. *J. Biol. Chem. 269*, 31491–31495.

(27) Laughrea, M., and Jette, L. (1996) HIV-1 Genome Dimerization: Formation Kinetics and Thermal Stability of Dimeric HIV-1Lai RNAs are Not Improved by the 1−232 and 296−790 Regions Flanking the Kissing-Loop Domain. *Biochemistry 35*, 9366–9374.

(28) Muriaux, D., Fosse, P., and Paoletti, J. (1996) A Kissing Complex Together with a Stable Dimer is Involved in the HIV-1Lai RNA Dimerization Process in Vitro. *Biochemistry 35*, 5075–5082.

(29) Muriaux, D., De Rocquigny, H., Roques, B. P., and Paoletti, J. (1996) NCp7 Activates HIV-1Lai RNA Dimerization by Converting a Transient Loop-Loop Complex into a Stable Dimer. *J. Biol. Chem. 271*, 33686–33692.

(30) Jalalirad, M., and Laughrea, M. (2010) Formation of Immature and Mature Genomic RNA Dimers in Wild-Type and Protease-Inactive HIV-1: Differential Roles of the Gag Polyprotein, Nucleocapsid Proteins NCp15, NCp9, NCp7, and the Dimerization Initiation Site. *Virology 407*, 225–236.

(31) Andersen, E. S., Contera, S. A., Knudsen, B., Damgaard, C. K., Besenbacher, F., and Kjems, J. (2004) Role of the Trans-Activation Response Element in Dimerization of HIV-1 RNA. *J. Biol. Chem. 279*, 22243–22249.

(32) Song, R., Kafaie, J., and Laughrea, M. (2008) Role of the 5′ TAR Stem−Loop and the U5-AUG Duplex in Dimerization of HIV-1 Genomic RNA. *Biochemistry 47*, 3283–3293.

(33) Hoglund, S., Ohagen, A., Goncalves, J., Panganiban, A. T., and Gabuzda, D. (1997) Ultrastructure of HIV-1 Genomic RNA. *Virology 233*, 271–279.

(34) Laughrea, M., Shen, N., Jette, L., Darlix, J. L., Kleiman, L., and Wainberg, M. A. (2001) Role of Distal Zinc Finger of Nucleocapsid Protein in Genomic RNA Dimerization of Human Immunodeficiency Virus Type 1; no Role for the Palindrome Crowning the R-U5 Hairpin. *Virology 281*, 109–116.

(35) Loweth, C. J., Caldwell, W. B., Peng, X. G., Alivisatos, A. P., and Schultz, P. G. (1999) DNA-Based Assembly of Gold Nanocrystals. *Angew. Chem., Int. Ed. 38*, 1808–1812.

(36) Jakobsen, M. R., Damgaard, C. K., Andersen, E. S., Podhajska, A., and Kjems, J. (2004) A Genomic Selection Strategy to Identify Accessible and Dimerization Blocking Targets in the 5′-UTR of HIV-1 RNA. *Nucleic Acids Res. 32*, e67.

(37) Pallesen, J., Dong, M., Besenbacher, F., and Kjems, J. (2009) Structure of the HIV-1 Rev Response Element Alone and in Complex with Regulator of Virion (Rev) Studied by Atomic Force Microscopy. *FEBS J. 276*, 4223–4232.

(38) Santos, N. C., and Castanho, M. A. (2004) An Overview of the Biophysical Applications of Atomic Force Microscopy. *Biophys. Chem. 107*, 133–149.

(39) Abbink, T. E., Beerens, N., and Berkhout, B. (2004) Forced Selection of a Human Immunodeficiency Virus Type 1 Variant that Uses a Non-Self tRNA Primer for Reverse Transcription: Involvement of Viral RNA Sequences and the Reverse Transcriptase Enzyme. *J. Virol. 78*, 10706–10714.

(40) Beerens, N., Groot, F., and Berkhout, B. (2001) Initiation of HIV-1 Reverse Transcription is Regulated by a Primer Activation Signal. *J. Biol. Chem. 276*, 31247–31256.

(41) Beerens, N., and Berkhout, B. (2002) The tRNA Primer Activation Signal in the Human Immunodeficiency Virus Type 1 Genome is Important for Initiation and Processive Elongation of Reverse Transcription. *J. Virol. 76*, 2329–2339.

(42) Ooms, M., Cupac, D., Abbink, T. E., Huthoff, H., and Berkhout, B. (2007) The Availability of the Primer Activation Signal (PAS) Affects the Efficiency of HIV-1 Reverse Transcription Initiation. *Nucleic Acids Res. 35*, 1649–1659.

(43) Tanigawa, M., and Okada, T. (1998) Atomic Force Microscopy of Supercoiled DNA Structure on Mica. *Anal. Chim. Acta 365*, 19–25.

(44) Paillart, J. C., Skripkin, E., Ehresmann, B., Ehresmann, C., and Marquet, R. (2002) In Vitro Evidence for a Long Range Pseudoknot in the 5′-Untranslated and Matrix Coding Regions of HIV-1 Genomic RNA. *J. Biol. Chem. 277*, 5995–6004.

(45) Miyazaki, Y., Irobalieva, R. N., Tolbert, B. S., Smalls-Mantey, A., Iyalla, K., Loeliger, K., D'Souza, V., Khant, H., Schmid, M. F., Garcia, E. L., Telesnitsky, A., Chiu, W., and Summers, M. F. (2010) Structure of a Conserved Retroviral RNA Packaging Element by NMR Spectroscopy and Cryo-Electron Tomography. *J. Mol. Biol. 404*, 751–772.

(46) Lear, A. L., Haddrick, M., and Heaphy, S. (1995) A Study of the Dimerization of Rous Sarcoma Virus RNA in Vitro and in Vivo. *Virology 212*, 47–57.

(47) Ortiz-Conde, B. A., and Hughes, S. H. (1999) Studies of the Genomic RNA of Leukosis Viruses: Implications for RNA Dimerization. *J. Virol. 73*, 7165–7174.